Second Harmonic Generation of Lamb Wave in Numerical Perspective *

Wu-Jun Zhu(朱武军)[1], Ming-Xi Deng(邓明晰)[2], Yan-Xun Xiang(项延训)[1**],
Fu-Zhen Xuan(轩福贞)[1], Chang-Jun Liu(刘长军)[1]

[1]*Key Laboratory of Pressure Systems and Safety of MOE, School of Mechanical and Power Engineering, East China University of Science and Technology, Shanghai 200237*
[2]*Department of Physics, Logistics Engineering University, Chongqing 401331*

(Received 12 June 2016)

The influences of phase and group velocity matching on cumulative second harmonic generation of Lamb waves are investigated in numerical perspective. Finite element simulations of nonlinear Lamb wave propagation are performed for Lamb wave mode pairs with exact and approximate phase velocity matching, with and without group velocity matching, respectively. The evolution of time-domain second harmonic Lamb waves is analyzed with the propagation distance. The amplitudes of primary and second harmonic waves are calculated to characterize the acoustic nonlinearity. The results verify that phase velocity matching is necessary for generation of the cumulative second harmonic Lamb wave in numerical perspective, while group velocity matching is demonstrated to not be a necessary condition.

PACS: 43.25.+y, 43.35.+d DOI: 10.1088/0256-307X/33/10/104301

Compared with traditional linear waves, nonlinear Lamb waves have been widely found to be sensitive to lattice anharmonicity and microstructural evolution in large plate-like structures due to the distortion of ultrasound, which make it a powerful tool to quantitatively characterize material degradation for nondestructive evaluation and structural health monitoring.[1–10] A Lamb wave can usually be transmitted and received on the same side with higher inspection efficiency than traditional bulk waves. However, due to the inherent dispersive and multimode natures of Lamb waves, generation of cumulative second harmonic Lamb waves (SHLWs) is only possible under certain conditions of phase velocity matching and non-zero energy flux.[1–3] When a Lamb wave propagates with a finite duration in practical measurement, an additional condition of group velocity matching is still contradictory.[11–13] Due to the mathematical complexity, analytical solutions related to group velocity of nonlinear wave equation are difficult to obtain. The influence of approximate phase velocity matching and group velocity mismatching on second harmonic generation is always limited in experimental investigation due to the attenuation and diffraction loss in materials and multimode characteristic of the Lamb wave. Furthermore, although most previous research has focused on theoretical and experimental investigations, few works are available with respect to numerical analyses.[14–16] Therefore, the influences of phase and group velocity matching on cumulative SHLW generation are necessarily further investigated in numerical perspective, since finite element (FE) simulation can provide the physical process of nonlinear Lamb wave propagation without mathematical complexity. In this letter, FE simulations of nonlinear Lamb wave propagation are carried out for Lamb wave mode pairs with exact and approximate phase velocity matching, with and without group velocity matching, respectively.

Based on the modal analysis approach,[17] SHLWs are generated by the bulk driving force in the interior of the plate and the traction stress at the upper and bottom surfaces of the plate due to the material and convective nonlinearities, which are contained in the nonlinear constitutive relation expressed as[18]

$$P_{ij} = C_{ijkl}\frac{\partial u_k}{\partial X_l} + \frac{1}{2}(C_{ijklmn} + C_{ijln}\delta_{km} + C_{jnkl}\delta_{im} + C_{jlmn}\delta_{ik})\frac{\partial u_k}{\partial X_l}\frac{\partial u_m}{\partial X_n}, \quad (1)$$

where P_{ij} is the first Piola–Kirchhoff stress tensor, u_i is the particle displacement vector, X_l is the Lagrangian coordinate, and C_{ijkl} and C_{ijklmn} are the second- and third-order elastic tensors defined as

$$C_{ijkl} = \lambda\delta_{ij}\delta_{kl} + 2\mu I_{ijkl}, \quad (2)$$

$$C_{ijklmn} = \frac{A}{2}(\delta_{ik}I_{jlmn} + \delta_{il}I_{jkmn} + \delta_{jk}I_{ilmn} + \delta_{jl}I_{ikmn}) + 2B(\delta_{ij}I_{klmn} + \delta_{kl}I_{mnij} + \delta_{mn}I_{ijkl}) + 2C\delta_{ij}\delta_{kl}\delta_{mn}, \quad (3)$$

where λ and μ are the Lamb constants, A, B and C are the third-order elastic constants, δ_{ij} is Kronecker's delta and $I_{ijkl} = (\delta_{ik}\delta_{jl} + \delta_{il}\delta_{jk})/2$.

FE simulations of nonlinear Lamb wave propagation in a 2-mm-thick titanium alloy plate are performed using the commercial software Abaqus/EXPLICIT. Figure 1 illustrates the schematic diagram of the 2D plane strain model with no attenuation and dispersion. The length of the isotropic and homogenous plate is 600 mm. The upper and bottom surfaces are assumed to be traction-free. The dispersion curves are shown in Fig. 2, where the red and

*Supported by the National Natural Science Foundation of China under Grant Nos 51325504, 11474093, 11622430 and 11474361, the National Key Research and Development Program of China (2016YFC0801903-02), and the Fundamental Research Funds for the Central Universities.

**Corresponding author. Email: yxxiang@ecust.edu.cn

© 2016 Chinese Physical Society and IOP Publishing Ltd

blue curves represent the symmetric and antisymmetric primary Lamb waves, respectively, and the black curves represent the symmetric SHLWs with half the frequency. Note that Lamb wave mode pair S1–s2 at point 1 satisfies the condition of phase and group velocity matching at 1.774 MHz, while Lamb wave mode pair S2–s4 at point 2 satisfies the condition of phase velocity matching and group velocity mismatching at 2.51 MHz.

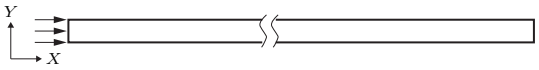

Fig. 1. Schematic diagram of the titanium alloy plate.

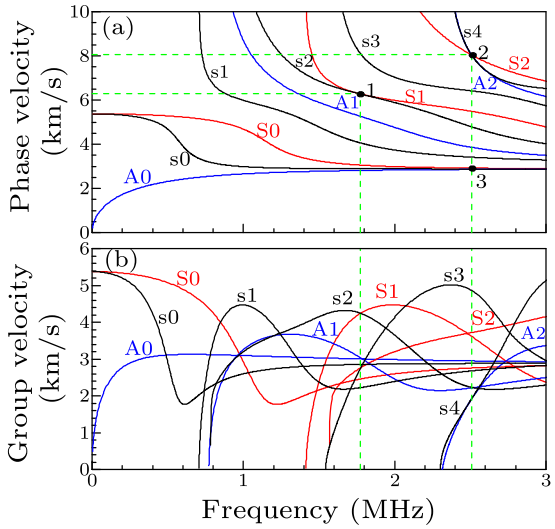

Fig. 2. Dispersion curves of Lamb waves propagating in a 2-mm-thick titanium plate for (a) phase velocity and (b) group velocity.

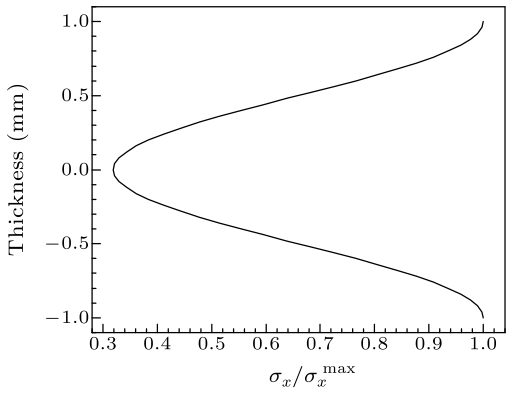

Fig. 3. Thickness profile of the longitudinal stress of S1 mode at 1.774 MHz.

The inherent elastic nonlinearity is introduced into the model through incorporating the nonlinear constitutive relation (1) into a user-defined material subroutine VUMAT using FORTRAN. The model was mesh with plane strain elements CPE4R. To guarantee the simulation precision and error convergence, element size Δd should be smaller than the spatial resolution of λ/n, where λ is the wavelength of targeted Lamb mode, and n is a positive integer, which is assumed to be 24 in this work. To satisfy the stability analysis, the time step should be smaller than the time resolution of $\Delta d/c_{\rm p}$, where $c_{\rm p}$ is the phase velocity of targeted Lamb mode. This means that Lamb wave should not travel across an element in a step time.[19] The element size and time step used in the simulation are 0.02 mm and 2.6×10^{-9} s, respectively. The fundamental wave is excited at the left surface of the plate with the excitation stress $P_0A(t)B(Y)$, where P_0 is the amplitude, $A(t)$ is the temporal waveform, and $B(Y)$ is the thickness profile of the targeted Lamb wave, as shown in Fig. 3 for S1 mode at 1.774 MHz. Unintended Lamb modes would be suppressed due to the given thickness profile. Here P_0 is chosen to be 20 MPa, as the amplitude of a few MPa is typical for Lamb wave propagation in solid. The computed longitudinal stress is picked to extract the time-domain received signal.

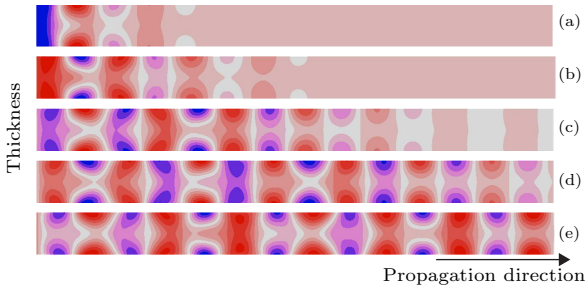

Fig. 4. Snapshots of longitudinal stress evolution at times (a) 4, (b) 6, (c) 8, (d) 10 and (e) 12 μs.

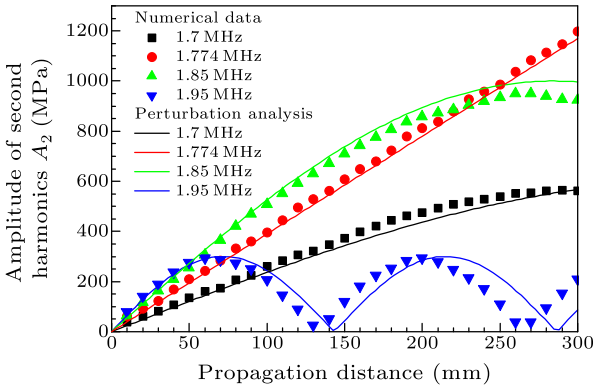

Fig. 5. Amplitude of second harmonic Lamb wave versus propagation distance for mode pair S1–s2.

The influence of phase velocity matching on the generation of cumulative SHLW is investigated firstly. Nonlinear Lamb wave propagation is simulated for mode pair S1–s2 at point 1 in Fig. 2. The fundamental wave is stimulated continually at 1.774 MHz, where phase and group velocity matchings are satisfied. The snapshots of longitudinal stress evolution are shown in Fig. 4. To interrogate the role of approximate phase velocity matching on the generation of SHLW, nonlinear simulations are further conducted at the fundamental frequencies of 1.7, 1.85 and 1.95 MHz, where both the phase and group velocities of primary Lamb waves are slightly different from those of SHLWs. To guarantee sufficient signal-to-noise ra-

tio, receivers are placed at nodes at the upper surface located in the range 10–300 mm away from the excitation source with an interval of 10 mm, since the longitudinal stress is largest through the thickness at surfaces. Due to the dispersive and multi-mode nature of Lamb waves, time-frequency analysis is needed to separate the individual mode contributions from the complicated time-domain signals. Short-time Fourier transform (STFT) is performed on the time-domain received signals to extract the amplitude of SHLWs as A_2.

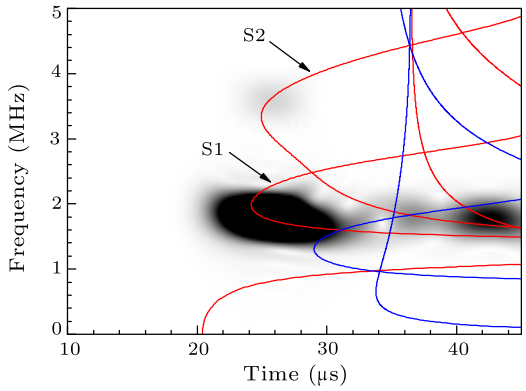

Fig. 6. Frequency–time spectrogram integrated with dispersion curves of group velocity.

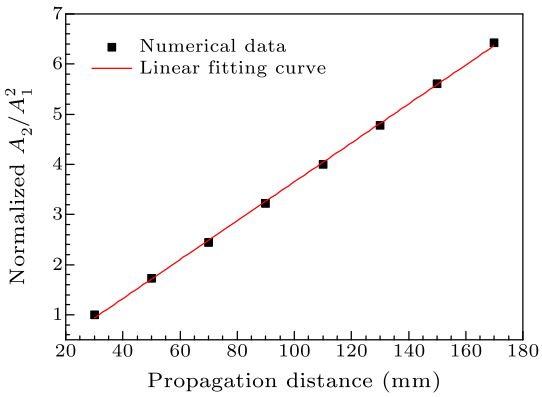

Fig. 7. Normalized ultrasonic nonlinearity parameter versus propagation distance for mode pair S1–s2.

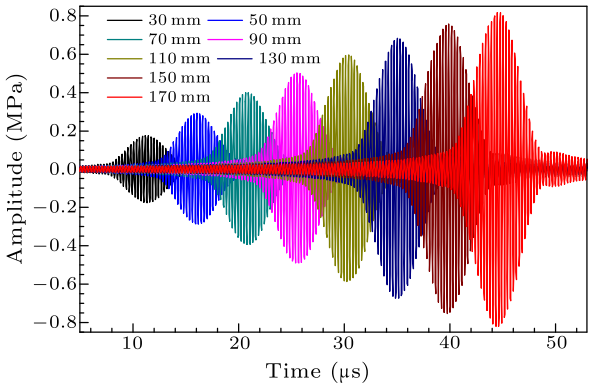

Fig. 8. Time-domain presentation of the second harmonic for mode pair S1–s2.

The amplitude of SHLWs, A_2, is plotted as a function of the propagation distance for mode pair S1–s2, as shown in Fig. 5. The points represent the results of simulation, while the curves are calculated by the perturbation analysis. Here A_2 increases linearly with the propagation distance at the matching frequency of 1.774 MHz. However, A_2 oscillates with the propagation distance at neighboring frequencies. Furthermore, both the propagation distance, within which A_2 grows cumulatively, and the maximum amplitude decreases with the difference between the matching and excitation frequency. Consequently, it is numerically verified that while approximate phase velocity matching is appropriate for cumulative SHLW generation within a limited propagation distance, exact phase velocity matching is necessary for linear increase of ultrasonic nonlinearity.

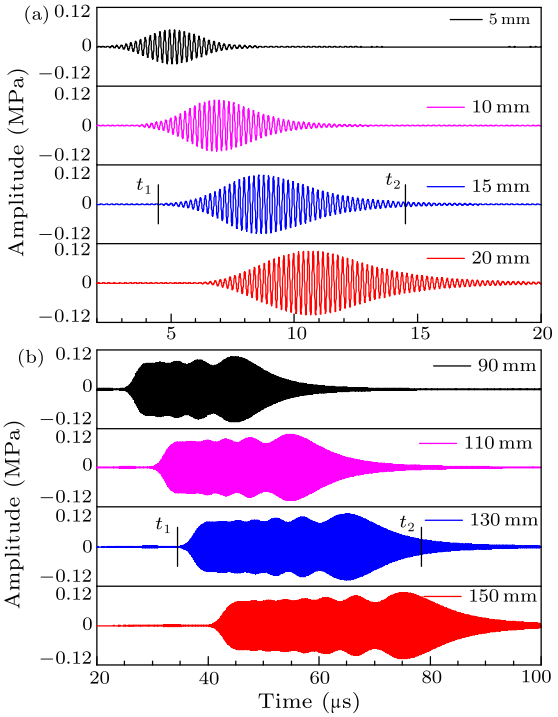

Fig. 9. Time-domain presentation of the second harmonic for mode pair S2–s4 in (a) stage I and (b) stage II.

To investigate the influence of group velocity matching on cumulative SHLW generation, FE simulations of nonlinear Lamb wave propagation are performed for mode pair S1–s2 at point 1 and mode pair S2–s4 at point 2 in Fig. 2. Note that both the mode pairs satisfy the condition of phase velocity matching, while group velocity matching is only satisfied for the mode pair S1–s2. The fundamental wave is modulated by 15 cycles Hanning-windowed sinusoidal tone bursts. For mode pair S1–s2, the fundamental wave is excited at 1.774 MHz. Receivers are placed at nodes at the upper surface located from 30 to 170 mm away from the excitation source with an interval of 20 mm. The frequency spectra of the receiving signals are extracted by using the STFT, as shown in Fig. 6. The amplitudes of primary Lamb waves and SHLWs, A_1 and A_2, are obtained. The acoustic nonlinearity parameter is calculated as A_2/A_1^2. As shown in Fig. 7, normalized A_2/A_1^2 grows linearly with the propagation distance. The pulse-inversion technique is applied to

extract the time-domain SHLW.[20] Nonlinear Lamb wave propagation is simulated with 0° and 180° out-of-phase inputs, respectively. The time-domain SHLW is acquired by superposing the corresponding received signals, as shown in Fig. 8. The amplitude of SHLW increases linearly with the propagation distance with a fixed duration.

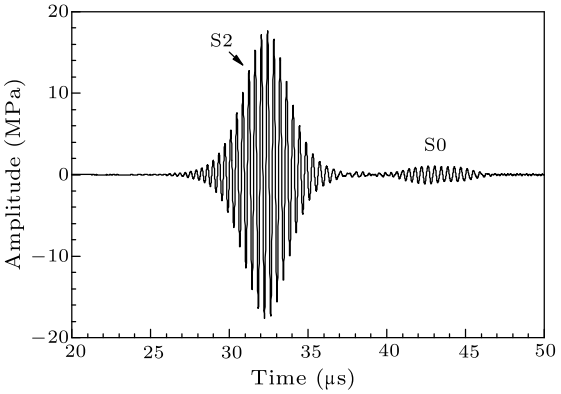

Fig. 10. Time-domain presentation of a typical received signal.

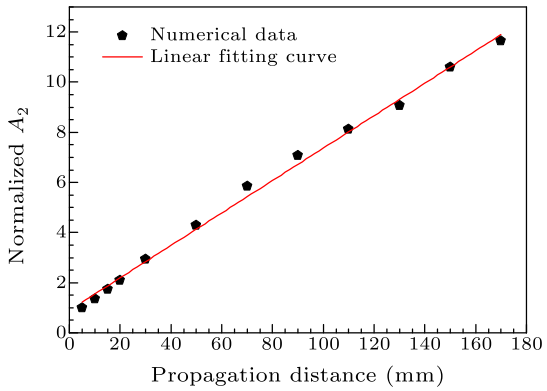

Fig. 11. Normalized amplitude of the second harmonic versus propagation distance for mode pair S2–s4.

For mode pair S2–s4, the fundamental wave is stimulated at 2.51 MHz. The time-domain SHLW is also obtained through the pulse-inversion technique. It is found that the evolution of SHLW envelope is divided into two stages (stages Ⅰ and Ⅱ) by a critical propagation distance $z_c = \tau c_g^f c_g^{2f}/(c_g^f - c_g^{2f})$, where c_g^f and c_g^{2f} are the group velocities of the primary Lamb wave and the SHLW, respectively, and τ is the duration of excited signal.[13] The critical distance is calculated to be 24.15 mm in this work. Receivers are placed at nodes in the middle plane located from 5 to 20 mm with an interval of 5 mm in stage Ⅰ, and from 30 to 170 mm with an interval of 20 mm in stage Ⅱ. The evolution of the time-domain SHLW is illustrated in Fig. 9. In stage Ⅰ, the envelope of the SHLW is a bit like a Hanning window. The maximum amplitude of the envelope grows cumulatively with the propagation distance with a linearly increasing duration. In stage Ⅱ, the envelope of the SHLW is a bit like the shape of a crystal. The amplitude of the envelope keeps almost constant with the propagation distance in a linearly increasing duration. The slight oscillation may be attributed to the unintended mode pair S0–s0 at point 3 in Fig. 2. As shown in Fig. 10, S0 mode was generated, since the thickness profile of the S0 mode is a bit similar to that of the S2 mode at the fundamental frequency. The tail-like part may be ascribed to the ring effect. The time-domain SHLW at propagation distance z mainly ranges from $t_1 = z/c_g^f$ to $t_2 = z/c_g^{2f} + \tau$.[13] Considering the increasing duration, fast Fourier transform (FFT) is performed on the signals from t_1 to t_2. The magnitude A_2 is extracted as an accumulation of SHLWs. As shown in Fig. 11, A_2 grows linearly with the propagation distance.

In conclusion, for nonlinear Lamb wave excited continually, the amplitude of SHLW oscillates with the propagation distance under the condition of approximate phase velocity matching and grows linearly when exact phase velocity matching is satisfied. Furthermore, for the fundamental wave with a finite duration, the acoustic nonlinearity grows linearly with the propagation distance in a fixed duration under the condition of group velocity matching. When group velocity mismatching is satisfied, both the duration and the maximum amplitude of the time-domain SHLW grow cumulatively with the propagation distance in stage Ⅰ. The duration increases linearly with an almost constant amplitude in stage Ⅱ. Whether group velocity matching is satisfied or not, the magnitude of the SHLW grows linearly with the propagation distance. It is verified numerically that phase velocity matching is necessary for cumulative SHLW generation, while group velocity matching is not a necessary condition.

References

[1] Deng M X 1999 *J. Appl. Phys.* **85** 3051
[2] de Lima W J N and Hamilton M F 2003 *J. Sound Vib.* **265** 819
[3] Deng M X 2003 *J. Appl. Phys.* **94** 4152
[4] Kim C S and Jhang K Y 2012 *Chin. Phys. Lett.* **29** 060702
[5] Liu Y, Chillara V K and Lissenden C J 2013 *J. Sound Vib.* **332** 4517
[6] Xiang Y X, Deng M X, Xuan F Z, Chen H and Chen D Y 2012 *Chin. Phys. Lett.* **29** 106202
[7] Xiang Y X, Zhu W J, Liu C J, Xuan F Z, Wang Y N and Kuang W C 2015 *NDTE Int.* **72** 41
[8] Cantrell J H and Yost W T 2013 *J. Appl. Phys.* **113** 153506
[9] Sagar S P, Metya A K, Ghosh M and Sivaprasad S 2011 *Mater. Sci. Eng.* A **528** 2895
[10] Pau A and Lanza di Scalea F 2015 *J. Acoust. Soc. Am.* **137** 1529
[11] Matsuda N and Biwa S 2011 *J. Appl. Phys.* **109** 094903
[12] Muller M F, Kim J Y, Qu J and Jacobs L J 2010 *J. Acoust. Soc. Am.* **127** 2141
[13] Deng M X, Xiang Y X and Liu L B 2011 *J. Appl. Phys.* **109** 113525
[14] Zhu W J, Deng M X, Xiang Y X, Xuan F Z and Liu C J 2016 *Ultrasonics* **68** 134
[15] Matsuda N and Biwa S 2012 *Jpn. J. Appl. Phys.* **51** 07GB14
[16] Hong M, Su Z Q, Wang Q, Li C and Qing X L 2014 *Ultrasonics* **54** 770
[17] Auld B 1973 *Acoustic Fields and Wave in Solids* (New York: Wiley)
[18] Hamilton M F and Blackstock D T 1998 *Nonlinear Acoustics* (New York: Academic)
[19] Sewell G 2005 *The Numerical Solution of Ordinary and Partial Differential Equations* (New York: Wiley)
[20] Kim J Y, Jacobs L J, Qu J and Littles J W 2006 *J. Acoust. Soc. Am.* **120** 1266